Anal. Chem. **1998,** *70,* 4004−4014

Influence of the Hapten Design on the Development of a Competitive ELISA for the Determination of the Antifouling Agent Irgarol 1051 at Trace Levels

Berta Ballesteros,[†,‡] Damià Barceló,[‡] Francisco Sanchez-Baeza,[†] Francisco Camps,[†] and María-Pilar Marco*[,†]

Departments of Biological Organic Chemistry and Environmental Chemistry, C.I.D.−C.S.I.C., Jorge Girona, 18-26, Barcelona, Spain

Enzyme-linked immunosorbent assays (ELISAs) with a high detectability have been developed for determination of the antifouling agent Irgarol 1051. The features of the resulting assays have been rationalized by using molecular mechanic calculations (MM2+) to correlate the chemical structure of different immunizing haptens and the corresponding avidities of the obtained antisera. The ability of Irgarol 1051 to compete for the antibody binding sites with 11 horseradish peroxidase enzyme tracers, differing in the chemical structures of the hapten, has been investigated. The present paper demonstrates that high-quality antibodies and, therefore, immunoassays reaching very low detection limits could be predicted by molecular modeling studies of the analyte conformations and of the immunizing haptens' geometries, hydrogen-bonding capabilities, and electronic distributions. Two of the ELISAs obtained have been optimized to obtain reproducible immunoassays. The dynamic ranges of both assays are between 30 and 200 ng/L, and the limits of detection are ∼16 ng/L. The reported immunoassays have been evaluated and validated by analyzing spiked and real seawater samples. Irgarol 1051 has been found to be present in two of the geographical locations analyzed at concentration levels dependent on the time of year. The analytical results obtained with these immunoassays have been validated by chromatographic methods.

Pilot survey studies of coastal water contamination have been so far mainly focused on tributyltin (TBT), which has recently been restricted after the regulations introduced by the European Community and the Mediterranean region.[1,2] The herbicide Irgarol 1051 [2-(methylthio)-4-(*tert*-butylamino)-6-(cyclopropylamino)-*s*-triazine] has replaced this agent as the biocide in antifouling paints in combination with copper- and zinc-based agents. As with other triazines, Irgarol 1051 is mainly present in the dissolved phase. However, its low solubility in water (Irgarol 1051, 7 mg/L; atrazine 33 mg/L; terbutryn 25 mg/L)) and high partition coefficient (Irgarol 1051 $K_{oc} = 3.0$; atrazine $K_{oc} = 2.1$; terbutryn $K_{oc} = 2.8$)[3] explains its reported association with sediments.[3] Regarding its undesirable effects over the aquatic environment, it has been reported by long-term studies that a significant decrease of the photosynthetic activity of the periphyton occurs at concentrations ranging from 0.25 to 1 nM (0.063−0.25 μg/L). On the other hand, it is worth noting the reported toxicity of Irgarol 1051 in the rainbow trout assay with an EC_{50} of 0.86 mg/L, 10-fold higher than that of the atrazine.[4]

Before 1992, contamination of coastal waters by Irgarol 1051 was unknown. The first report pointing to the presence of this agent on the coastline of the Côte d'Azur at concentrations ranging from 0.11 to 1.7 μg/L appeared in 1993.[5] One year later, coastal water contamination by Irgarol 1051 was also found in southern England at slightly lower, but still significant, concentrations (0.002−0.5 μg/L).[6] Recently, the presence of Irgarol 1051 was observed in other regions of Europe such as the western coast of Sweden[7] and the freshwater lake of Geneve.[4] Similarly, we have also found contamination by Irgarol 1051 on the Mediterranean Spanish coast.[8]

The methods of analysis applied to Irgarol 1051 determination are common to other triazines: GC/NPD (gas chromatography with nitrogen and phosphorus detector), GC/MS (mass spectrometry detection), HPLC/DAD (high-performance liquid chromatography with diode array detection), or HPLC/MS that reaches very low detection limits (5 ng/L) by preconcentrating high sample volumes (0.5−1 L). It is known that, among other benefits, immunoassays are able to simultaneously process many

* Corresponding author: (phone) 34 93 400 61 00; (fax) 34 93 204 59 04; (e-mail) mpmqob@cid.csic.es.

† Department of Biological Organic Chemistry.

‡ Department of Environmental Chemistry.

(1) UNEP; UNEP(OCA)/MED IG. 1/5, 1989.

(2) Europeenne, C.; European Community: Journal officiel des Communautes Europeennes, 1989; pp 19−23.

(3) Tolosa, I.; Readman, J. W.; Blaevoet, A.; Ghilini, S.; Bartocci, J.; Horvat, M. *Mar. Pollut. Bull.* **1996**, *32*, 335−341.

(4) Toth, S.; Becker-van Slooten, K.; Spack, L.; de Alencastro, L. F.; Tarradellas, J. *Bull. Environ. Contam. Toxicol.* **1996**, *57*, 426−433.

(5) Readman, J. W.; Liong Wee Kwong, L.; Gronding, D.; Bartocci, J.; Villeneuve, J.-P.; Mee, L. D. *Environ. Sci. Technol.* **1993**, *27*, 1940−1942.

(6) Gough, M. A.; Fothergill, J.; Hendrie, J. D. *Mar. Pollut. Bull.* **1994**, *28*, 613−620.

(7) Dahl, B.; Blanck, H. *Mar. Pollut. Bull.* **1996**, *32*, 342−350.

(8) Ferrer, I.; Ballesteros, B.; Marco, M.-P.; Barcelo, D. *Environ. Sci. Technol.* **1997**, *31*, 3530−3535.

S0003-2700(98)00241-8 CCC: $15.00
Published on Web 08/29/1998

samples reaching very low detection limits without need of cleanup or preconcentration steps, thus increasing throughput analysis. Water samples are ideal matrixes for immunoassay performance. Immunochemical methods have been demonstrated to be excellent screening tools for analyzing water samples with a high salt content (>35‰) such as seawater.[9] In studies on the coastal water contamination by Irgarol 1051, we have recently reported the development of an immunoassay[10] for the detection of this antifouling agent. Antibodies were raised against an immunogen prepared with a hapten lacking the cyclopropyl group of the molecule. The research presented in this paper deals with an improved immunoassay to analyze Irgarol 1051 in seawater environmental samples at very low concentration levels. It is known that immunoassay features are strongly determined by the chemical structure of the immunizing hapten.[11,12] Some authors have already discussed the usefulness of using computer molecular modeling studies of the haptens to predict their minimum energy conformations and rationalize immunoassay results.[13,14] In this work, molecular modeling studies (MM2+) have been used to interpret the obtained results and to establish a correlation between the sensitivity of the immunochemical analytical method and the participation of the different groups of the irgarol molecule in antibody binding.

EXPERIMENTAL SECTION

Thin-layer chromatography (TLC) was performed on 0.25-mm, precoated silica gel 60 F254 aluminum sheets (Merck, Gibbstown, NJ). ^{1}H and ^{13}C NMR spectra were run with a Varian Unity-300 spectrometer (300 MHz for ^{1}H and 75 MHz for ^{13}C) and the chemical shifts are expressed as δ, ppm. Infrared spectra were measured on a Bomen MB120 FT-IR spectrophotometer (Hartmann & Braun, Québec, Canada). Mass spectra were recorded on a MD-800 capillary gas chromatograph with MS quadrupole detector (Fisons Instruments, VG, Manchester, U.K.), and data are reported as m/z (relative intensity). The ion source temperature was set at 200 °C; a 15 m × 0.25 mm i.d. × 0.15 μm (film thickness) DB-225 fused-capillary column (J&W, Folsom, CA) was used; He was the carrier gas employed at 1 mL/min. GC conditions were as follows: temperature program, 60 to 90 °C (10 °C/min), 90 to 220 °C (6 °C/min), 220 °C (10 min); injector temperature, 250 °C. Hapten conjugates were analyzed by measuring their absorbance on a Uvikon 820 UV/visible spectrophotometer (Kontron, Zurich, Switzerland) on scan mode (200−400 nm). The matrix-assisted laser desorption/ionization mass spectrometer (MALDI-MS) used for analyzing the protein conjugates was a time-of-flight (TOF) mass spectrometer Bruker Biflex III (Bruker, Kalsruhe, Germany) equipped with a laser unit that operates at a wavelength of 337 nm and a maximum output of 6 mW. Polystyrene microtiter plates were purchased from Nunc (Maxisorb, Roskilde, Denmark). Washing steps were carried out using a SLY96 PW microplate washer (SLT Labinstruments GmbH, Salzburg, Austria). Absorbances were read using a Multikskan Plus MK II microplate reader (Labsystems) at a single-wavelength mode of 450 nm. The competitive curves were analyzed with a four-parameter logistic equation using the software Genesys (Labsystems Helsinki, Finland) and GraphPad Prism (GraphPad Sofware Inc., San Diego, CA). Unless otherwise indicated, data presented correspond to the average of at least two well replicates. Immunochemicals were obtained from Sigma Chemical Co. (St. Louis, MO). Chemical reagents were purchased from Aldrich Chemical Co. (Milwaukee, WI). Pesticide standards such as cyanazine, desmetryne, ametryne prometryne, propazine, terbutylazine, terbutrin, and terbumeton used for cross-reactivity studies were purchased from Riedel De Häen (Seelze, Germany) and Dr. Ehrenstorfer (Augsburg, Germany). Atrazine and simazine, used in synthesis, and Irgarol 1051, used as standard, were obtained as a gift from Ciba-Geigy (Barcelona, Spain).

Buffers. PBS is 0.2 M phosphate buffer, 0.8% saline solution and unless otherwise indicated the pH is 7.5. PBS−BSA is PBS containing a 0.1% of BSA. Borate buffer is 0.2 M boric acid−sodium borate, pH 8.7. Coating buffer is 0.5 M carbonate−bicarbonate buffer, pH 9.6. PBST is 0.2 M phosphate buffer, 0.8% saline solution, 0.05% Tween 20. PBST at double concentration is 2× PBST. Citrate buffer is a 0.1 M solution of sodium citrate, pH 5.5. The substrate solution contains 0.01% 3,3′,5,5′-tetramethylbenzidine (TMB; *handle with care*, *carcinogenic compound*) and 0.004% H_2O_2 in citrate buffer.

Molecular Modeling. The calculations were performed using the Hyperchem 4.0 software package (Hyperube Inc., Gainesville, FL). Theoretical geometries and electronic distributions were evaluated for Irgarol 1051 and related compounds such as terbumeton, propazine, and prometrine and for haptens **2a**, **4b**, **4c**, **4d**, and **4e** (all of them as amide derivatives). The eight main conformers possible for each of them (defined by the relative orientation of the triazine ring substituents) were fully optimized using molecular mechanics model MM+ for the minimum energy levels. These final geometries were used as starting points in the semiempirical quantum mechanical model PM3 calculations. Molecular electronic distributions were derived from the last model.

Synthesis of the Haptens. The chemical structures of the haptens used in this paper are shown in Table 1. The preparation of haptens **2e** and **4d** has been previously described.[10] The synthesis of the carboxylic acid derivatives of atrazine (**2b**, **2d**, **4a**) and simazine (**2a**, **2c**, **4b**) has been reported.[15] Haptens **2f**, **4c**, and **4e** were prepared as follows.

(4,6-Dichloro[1,3,5]triazin-2-yl)cyclopropylamine (1d). Following similar procedures as already described,[10,15] cyclopropylamine (3.9 mg, 56 mmol) was reacted with cyanuric chloride (10 g, 54.2 mmol) in the presence of *N*,*N*-diisopropylethylamine (9.75 mL, 56 mmol) in diethyl ether (450 mL) to provide 10.07 g (91% yield) of crystalline **1d**: IR (KBr, cm^{-1}) 3428 (st N−H), 3143, 3095, and 3016 (st C−H), 1592 (δ HN<), 1565 and 1544 (st C=

(9) Gascon, J.; Oubiña, A.; Onnefjord, P.; Ferre, I.; Hammock, B. D.; Marko-Varga, G.; Marco, M.-P.; Barceló, D. *Anal. Chim. Acta* **1996**, *330*, 41−51.

(10) Ballesteros, B.; Barcelo, D.; Camps, F.; Marco, M.-P. *Anal. Chim. Acta* **1997**, *347*, 139147.

(11) Marco, M.-P.; Gee, S.; Hammock, B. D. *Trends Anal. Chem.* **1995**, *14*, 415−425.

(12) Szurdoki, F.; Bekheit, H. K. M.; Marco, M.-P.; Goodrow, M. H.; Hammock, B. D. In *New Frontiers in Agrochemical Immunoassay*; Kurtz, D. A., Skerritt, J. H., Stanker, L., Eds.; AOAC International: Arlington, VA, 1995; pp 39−63.

(13) Holtzapple, C. K.; Carlin, R. J.; Rose, B. G.; Kubena, L. F.; Stanker, L. H. *Mol. Immunol.* **1996**, *33*, 939−946.

(14) Lee, N. J.; Skerritt, J. H.; McAdam, D. P. *J. Agric. Food Chem.* **1995**, *43*, 1730−1739.

(15) Gascón, J.; Ballesteros, B.; Oubiña, A.; Gonzalez- Martinez, M.-P.; Puchades, R.; Maquieira, A.; Marco, M.-P.; Barceló, D. *Anal. Chim. Acta* **1997**, *347*, 149−162.

Table 1. Homology of the Chemical Structures of the Haptens Used as Enzyme Tracers with the Target Analyte Irgarol 1051[a]

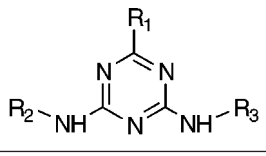

	hapten	R_1	R_2	R_3
group I	**2a**	Cl	ethyl	$(CH_2)_3COOH$
	2b	Cl	isopropyl	$(CH_2)_3COOH$
	2c	Cl	ethyl	$(CH_2)_3COOH$
	2d	Cl	isopropyl	$(CH_2)_3COOH$
group II	**2e**	Cl	*tert-butyl*	$(CH_2)_3COOH$
	2f	Cl	$(CH_2)_3COOH$	*cyclopropyl*
	4a	*$S(CH_2)_2COOH$*	ethyl	ethyl
	4b	*$S(CH_2)_2COOH$*	isopropyl	ethyl
group III	**4d**	*SCH_3*	*tert-butyl*	$(CH_2)_3COOH$
	4e	*SCH_3*	$(CH_2)_3COOH$	*cyclopropyl*
group IV	**4c**	*$S(CH_2)_2COOH$*	*tert-butyl*	*cyclopropyl*
target analyte	*Irgarol 1051*	*SCH_3*	*tert-butyl*	*cyclopropyl*

[a] Italic type entry indicates homology with the target analyte.

N) 1509 (st C_{Ar}−N), 1453 and 1394 (δ sy CH_2); ^{1}H NMR (300 MHz, $CDCl_3$, δ ppm) 0.57 (m, 2H, CH_2 cyclopropyl), 0.87 (m, 2H, CH_2 cyclopropyl), 2.80 (m, 1H, CHN), 6.23 (br s, 1H, NH); ^{13}C NMR (75 MHz, $CDCl_3$, δ, ppm) 7.33 (CH_2), 24.05 (CH), 167.22 (CN_3), 169.61 (CN_2Cl), 171.11 (CN_2Cl); EIMS m/z (relative intensity) 204 ($M^{\bullet+}$, 10), 189 ($M^{\bullet+} - CH_3$, 100). Anal. Calcd for $C_6H_6N_4Cl_2$ (205.05): C, 35.15; H, 2.95; N, 27.32; Cl, 34.58. Found: C, 35.22; H, 3.10; N, 27.27; Cl, 34.54.

4-[*N*-4-Cyclopropylamino)-6-chloro[1,3,5]triazin-2-yl]aminobutyric Acid (2f). According to the procedures already described for similar compounds,[10,15] the triazine **1d** (3 g, 14.63 mmol) was reacted with 4-aminobutyric acid (1.66 g, 16.12 mmol) in the presence of *N*,*N*-diisopropylethylamine (5.1 mL, 14.63 mmol) in absolute ethanol (370 mL) for 14 h at room temperature and 5 h at reflux until complete disappearance of the starting material. Extraction of the reaction mixture yielded 1.27 g (32%) of pure **2f**: IR (KBr, cm^{-1}) 3267 (st N−H), 3282 (st O−H), 3128, 3093, 3012, and 2939 (st C−H), 1697 (st C═O), 1620 (δ HN<), 1589 and 1556 (st C═N), 1446 and 1407 (δ sy CH_2); ^{1}H NMR (300 MHz, DMSO-d_6, δ, ppm) 0.47 (m, 2H, CH_2 cyclopropyl), 0.63 (m, 2H, CH_2, cyclopropyl), 1.71 (m, J = 6.9, 2H, CH_2), 2.19 (m, 2H, CH_2COO), 2.72 (m, J = 3.9, 1H, CHN), 3.24 (m, 2H, 2 CH_2N), 7.83 (m, 2H, 2NH); ^{13}C NMR (75 MHz, DMSO-d_6, δ ppm) 5.82, 6.01 (2 CH_2, cyclopropyl), 23.32 (CH_2), 24.38 (CHN), 24.54 (CH_2-COO), 31.88 (CH_2N), 164.78 (CN_3), 165.43 (CN_3), 167.30 (CN_2-Cl), 174.59 (CO); methyl ester EIMS m/z (relative intensity) 285 ($M^{\bullet+}$, 85), 270 ($M^{\bullet+} - CH_3$, 100), 254 ($M^{\bullet+} - OCH_3$, 50), 238 (65), 226 ($M^{\bullet+} - COOCH_3$, 25), 212 ($M^{\bullet+} - CH_2COOCH_3$, 75), 198 ($M^{\bullet+} - (CH_2)_2COOCH_3$, 50).

2-(Cyclopropylamino)-6-chloro-4-(*tert*-butylamino)[1,3,5]-triazine (3c). Following the described synthetic methods,[15] cyclopropylamine (1.96 mL, 28.2 mmol) was reacted with **1c**[10] (6 g, 7.1 mmol) in the presence of *N*,*N*-diisopropylethylamine (4.92 mL, 28.2 mmol) in absolute ethanol (100 mL) to obtain 6.19 g (94% yield) of the desired product **3c**: IR (KBr, cm^{-1}) 3432 (st N−H), 3093, 2965, 2931, and 2868 (st C−H), 1573 and 1550 (st C═N), 1519 (st C_{Ar}−N), 1455, 1395, and 1380 (δ sy CH_2 and CH_3); ^{1}H NMR (200 MHz, $CDCl_3$, δ, ppm) 0.54 (m, 2H, CH_2, cyclopropyl), 0.76 (m, 2H, CH_2, cyclopropyl), 1.42 (s, 9H, 3 CH_3), 2.70 (m, 1H, CHN), 5.39 (br s, 1H, NH (cyclopropyl)), 6.25 (br s, 1H, NH (*tert*-butyl)); ^{13}C NMR (75 MHz, $CDCl_3$, δ, ppm) 7.11 (2 CH_2), 23.55 (CHN), 28.57 (3 CH_3), 51.59 ($(CH_3)_3CN$), 164.81 (CN_3), 166.72 (CN_3), 167.94 (CN_2Cl); EIMS m/z (relative intensity) 241 ($M^{\bullet+}$, 35), 226 ($M^{\bullet+} - CH_3$, 40), 184 ($M^{\bullet+} - Bu^t$, 25), 170 ($M^{\bullet+} - Bu^t - CH_2$, 100).

***S*-[4-(*tert*-Butylamino)-6-(cyclopropylamino)[1,3,5]triazin-2-yl]thiopropionic Acid (4c).** A solution of 3-mercaptopropionic acid (241 mg, 2.3 mmol) in 85% KOH (273 mg, 4.1 mmol), absolute degassed ethanol (20 mL) was added to a stirred solution of **3c** (0.5 g, 2.1 mmol) in the same solvent (20 mL) under argon atmosphere. The reaction mixture was treated according to the optimized procedure described before[15] to yield 416 mg of a yellow oil, which contained 80% of **4c** (51% yield) and 20% of the dithiopropionic acid (ratio determined by ^{1}H NMR). About 50 mg of the crude mixture was purified by reversed-phase chromatography (10 g of Isolute C_{18}) to obtain 30 mg of pure **4c**: IR (KBr, cm^{-1}) 3432 (st N−H), 3282 (st O−H), 3093, 2967, 2929, and 2871 (st C−H), 1710 (st C═O), 1556 (st C═N), 1519 (st C_{Ar}−N), 1453, 1409, and 1351 (δ sy CH_2 and CH_3); ^{1}H NMR (200 MHz, DMSO-d_6, δ, ppm) 0.48 (m, 2H, CH_2 cyclopropyl), 0.63 (m, 2H, CH_2 cyclopropyl), 1.36 (s, 9H, 3 CH_3), 2.63 (t, CH_2COO), 2.67 (m, J = 3.6, CHN), 3.14 (br s, 2H, CH_2S), 6.87 (s, 1H, NH), 7.46 (s, 1H, NH); ^{13}C NMR (75 MHz, DMSO-d_6, δ, ppm) 6.03 (2 CH_2), 20.97 (CHN), 23.18 (CH_2S), 28.68 (3CH_3), 34.53 (CH_2COOH), 50.23 ($(CH_3)_3CN$), 163.55 and 164.80 (2CN_3 and CNS), 171.82 (CO); methyl ester EIMS m/z (relative intensity) 325 ($M^{\bullet+}$, 90), 310 ($M^{\bullet+} - CH_3$, 45), 294 ($M^{\bullet+} - OCH_3$, 20), 268 (20), 254 ($M^{\bullet+} - COOCH_3$, 40), 238 (30), 224 (35), 210 (35), 182 (100).

4-[*N*-4-(Cyclopropylamino)-6-(methylthio)[1,3,5]triazin-2-yl]aminobutyric Acid (4e). A solution of sodium methanethiolate (258 mg, 3.7 mmol) in deoxygenated absolute ethanol (50 mL) was added under argon atmosphere to a stirred solution of **2f** (1 g, 3.7 mmol) in the same solvent (50 mL). The mixture was refluxed for 6 h. After 3 and 5 h, additional sodium methanethiolate (258 mg, 3.7 mmol) was added in ethanol (20 mL) until **2f** was no more detected by TLC analysis (hexane/diethyl ether/acetic acid, 5:2:0.01). The ethanol was removed under reduced pressure, and the residue was dissolved in 5% $NaHCO_3$ and washed with CH_2Cl_2. The aqueous layer was acidified with 1 N HCl to pH 3.9 to precipitate the acid **4e** and the suspension extracted with ethyl acetate. The organic layer was dried with Na_2SO_4 and filtered and the solvent evaporated to give 720 mg (69% yield) of the desired product **4e**: IR (KBr, cm^{-1}) 3429 (st N−H), 3280 (st O−H), 3131, 3011, 2956, and 2923 (st C−H), 1703 (st C═O), 1666 (δ HN<), 1552 (st C═N), 1510 (st C−N), 1479, 1450, and 1415 (δ sy CH_2 and CH_3); ^{1}H NMR (300 MHz, DMSO-d_6, δ, ppm) 0.46 (m, 2H, CH_2, cyclopropyl), 0.60 (m, 2H, CH_2, cyclopropyl), 1.71 (m, CH_2), 2.22 (t, J = 7.0, CH_2COO), 2.36 (s, CH_3S), 2.73 (m, CHN), 3.24 (m, CH_2N), 7.28 (br s, 2H, 2NH); ^{13}C NMR (75 MHz, DMSO-d_6, δ, ppm) 6.31 (2 CH_2), 14.51 (CH_3S), 23.39 (CH), 23.47 (CH_2), 24.81 (CH_2COO), 31.36 (CH_2N), 164.31 (CN_3), 165.35 (CN_3), 170.38 (CN_2S), 174.47 (CO); methyl ester EIMS m/z (relative intensity) 297 ($M^{\bullet+}$, 90), 282 ($M^{\bullet+}$ −

CH_3, 75), 266 ($M^{\bullet+}$ − OCH_3, 30), 224 ($M^{\bullet+}$ − CH_2COOCH_3, 25), 149 (100).

Conjugation to Carrier Proteins. (A) Antigens. Haptens **4c**, **4d**, and **4e** were covalently attached through the carboxylic acids to the lysine groups of keyhole limpet hemocyanin (KLH), bovine serum albumin (BSA), conalbumin (CONA), and ovalbumin (OVA) using the mixed anhydride method as previously described.[10] The conjugates were lyophilized and stored at −80 °C. Stock solutions of 1 mg/mL were prepared with PBS buffer and stored in aliquots at −20 °C. A working aliquot was kept a 4 °C.

(B) Enzyme Tracers (ETs). Haptens **2a**−**f** and **4a**−**e** were coupled to horseradish peroxidase (HRP) through their corresponding *N*-hydroxysuccinimide (NHS) esters using dicyclohexylcarbodiimide (DCC) as described.[15] Stock solutions (0.25 mg/mL) of these ETs were prepared in PBS−BSA/saturated $(NH_4)_2SO_4$ (1:1) and stored in aliquots under an argon atmosphere at 4 °C.

Hapten Density Analysis. Hapten densities of **4c**−**e**-BSA conjugates were determined by MALDI-TOF-MS by comparing the molecular weight of the standard BSA with that of the conjugates. MALDI spectra were obtained by mixing 2 μL of the matrix [(*E*)-3,5-dimethoxy-4-hydroxycinnamic acid, 10 mg/mL in CH_3CN/H_2O (70:30), 0.1% TFA] with 2 μL of a solution of the conjugates or proteins [10 mg/mL in CH_3CN/H_2O (70:30), 0.1% TFA]. Similar analysis could not be performed with the corresponding KLH conjugates used as immunogens because of the wide range of high molecular weights reported for this protein. Since both BSA and KLH conjugates were prepared simultaneously, a parallelism was assumed regarding the extent of the conjugation reactions.

Immunization of the Rabbits. Female New Zealand white rabbits weighing 2−4 kg were immunized with **4c**-KLH (rabbits 13, 14, and 15), **4d**-KLH (rabbits 16, 17, and 18), and **4e**-KLH (rabbits 19, 20, and 21) according to the immunization protocol already described.[15] Evolution of the antibody titer was assessed by measuring the binding of serial dilutions of the antisera to microtiter plates coated with **4c**-BSA, **4d**-BSA, or **4e**-BSA, respectively. Antiserum was obtained by centrifugation and stored at −80 °C in the presence of 0.02% NaN_3.

Screening of the Antisera (As) and ETs. The avidity of each antiserum for the different ETs was determined by measuring the binding of serial dilutions (1/1000 to 1/64000 in PBST, 100 μL/well) of the ETs **2a**−**f**-HRP and **4a**−**e**-HRP (1 h at room temperature) to microtiter plates coated (overnight, 4 °C) with 12 different dilutions of each sera (1/1000−1/256000 in coating buffer, 100 μL/well). Optimal concentrations for ETs and antisera were chosen to produce absorbances of 0.7−1 unit of absorbance in 30 min. With these concentrations, the ability of the analyte Irgarol 1051 to compete with the ETs for the antibody binding sites was investigated. These experiments were carried out by adding serial dilutions of the analyte (1000−0.002 nM in PBST, 50 μL/well) and the ETs (appropriately diluted in PBST, 50 μL/well) to the antisera-coated plates.

Optimized Competitive ELISAs. Microtiter plates were coated with the antiserum in coating buffer (As15 1/16000 or As16 1/8000, 100 μL/well) overnight at 4 °C, covered with adhesive plate sealers. The following day, the plates were washed 5 times with PBST buffer (300 μL/well). Serial dilutions of Irgarol (0.0037−100 nM in PBST) or samples were added to the coated plates (50 μL/well) and incubated for 45 min at room temperature. Subsequently, the ET (**4e**-HRP 1/8000 or **2a**-HRP 1/2000, respectively, in PBST, 50 μL/well) was added and incubated for 15 min more at room temperature. The plates were washed as described before and the substrate solution was added (100 μL/well). The enzymatic reaction was stopped after 30 min at room temperature with 50 μL of 4 M H_2SO_4, and the absorbances were read at 450 nm. The standard curve was fitted to a four-parameter logistic equation according to the following formula: $y = A - B/[1 + (x/C)^D] + B$,[16] where A is the maximal absorbance, B is the minimum absorbance, C is the concentration producing 50% of the maximal absorbance, and D is the slope at the inflection point of the sigmoid curve.

Cross-Reactivity Determinations. Stock solutions of different structurally related triazine pesticide were prepared (100 mM in DMSO) and stored at 4 °C. Standard curves were prepared in PBST (0.06−200 nM) and each IC_{50} determined in the competitive experiment described above. The cross-reactivity values were calculated according to the following equation: (I_{50}(irgarol)/I_{50}(triazine derivative)) × 100.

Matrix Effect Studies. Seawater (blank sample from Mediterranean open sea) and filtered seawater (0.45-μm filter) samples were used to prepare Irgarol 1051 standard curves and compare them to the curve prepared in MilliQ water. In these studies, the ET was diluted in 2× PBST. The competitive immunoassay was carried out as described above.

Analysis of Spiked and Real Sample Waters. Seasalt water was prepared by dissolving seasalts (Sigma Chemical Co.) to a concentration of 35‰ in MilliQ water. Environmental samples were collected in the Masnou Marina (Barcelona, Spain), Alfacs Bay, Fangar Bay (Ebre Delta, Tarragona, Spain), Jucar river, Albufera, Malvarosa, and Cullera (Valencia, Spain). Samples were buffered with 10% PBST 10×, and measured 1-, 2-, or 4-fold diluted by ELISA.

RESULTS AND DISCUSSION

Hapten Design and Synthesis. In our search for the best hapten molecule to obtain high-quality antisera, we investigated the MM2+ optimized geometry of Irgarol 1051. When calculations were carried out as usual (vacuum conditions), the eight conformers showed similar energies, which suggested similar molecular populations. The situation changed when the water dielectric constant and a network of water molecules was introduced in the MM+ model. In this case, one of the conformers appeared slightly more favored (~10 kJ/mol). This conformer had the two voluminous alkyl substituents oriented opposite to the methylthio group (see Figure 1A). The cyclopropyl group was placed perpendicularly outside of the plane defined by the triazine ring, which indicates a facial asymmetry. In contrast, the *tert*-butyl group covered an important space region more or less equally distributed on the two faces of the plane defined by the triazine ring. An interesting feature was the manifested accessibility of the two NH groups and of the two nitrogen atoms of the aromatic ring. This fact potentially allows the establishment of hydrogen bonds with other molecules such as the antibody or

(16) Tjissen, D. H. *Practice and Theory of Enzyme Immunoassays*; Elsevier: Amsterdam, 1985.

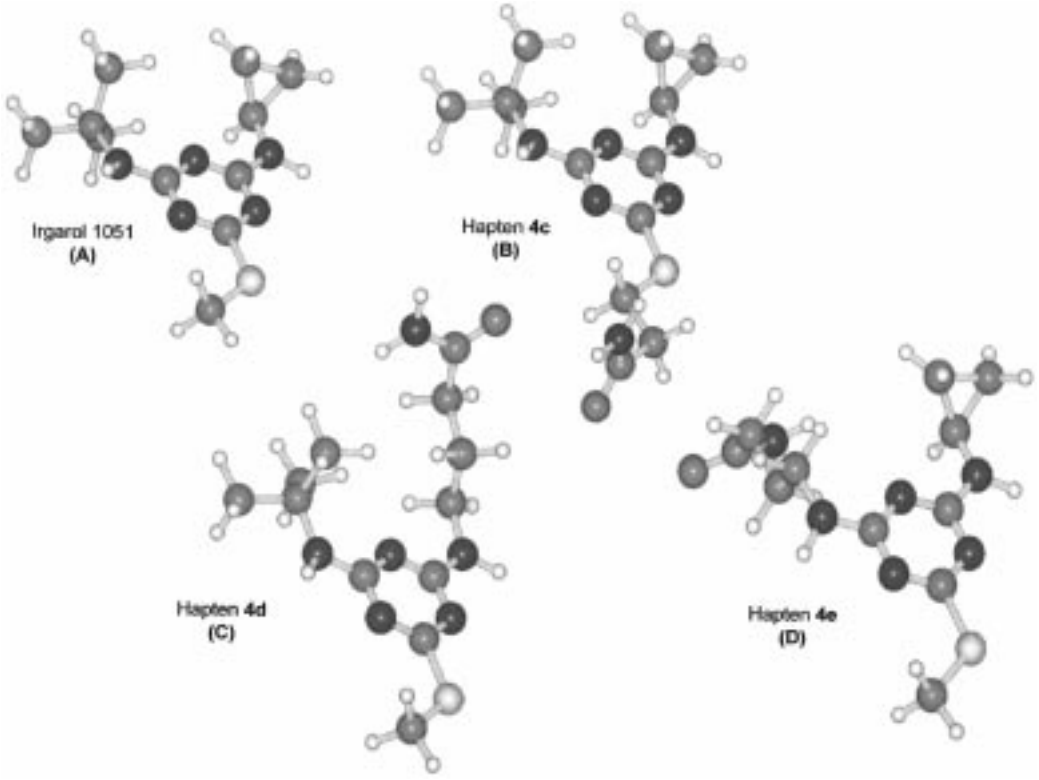

Figure 1. Ball and stick models of the minimum energy conformations of Irgarol 1051, haptens **4c**, **4d**, and **4e**, using molecular mechanics model MM+ and quantum mechanical model PM3 calculations. Calculations have been performed using the corresponding amide derivatives to mimic the conjugated hapten. Haptens **4c** and **4d** showed the greatest similarity to the analyte. The elements are presented in the following manner: light blue, carbon; dark blue, nitrogen; gray, hydrogen; yellow, sulfur; red, oxygen; and green, chlorine.

the solvent itself (see Figure 1A). Additionally, the aliphatic region limited by the *tert*-butyl and the cyclopropyl groups defines an asymmetric space area able to participate in hydrophobic interactions. Finally, the third position of the triazine ring, occupied by the methylthio group, confers special properties to the molecule due to the electronegativity and size of the sulfur atom.

In principle, high-affinity antibodies should afford immunochemical techniques with superior detectability. The molecular recognition relays on the molecular shape, defined by the geometry, and on low-energy interactions such as hydrogen bonding, hydrophobic interactions, and electrostatic and dipole−dipole forces together with $\pi-\pi$ complementary ring bonding. The preliminar analysis performed with the irgarol molecule suggested that all three groups could play an important role in the antibody binding and therefore a decision on which substituent had to be removed to place the spacer arm was difficult. For this reason, we addressed the synthetic preparation of three haptens (see Figure 2) to evaluate the participation of each of the substituents of the triazine ring in the antibody recognition. Analogously, by raising antisera against these three immunizing haptens, we would obtain a broader range of immunoassay selectivities.

The preparation of the haptens was accomplished by nucleophilic substitution of the chlorine atoms of the cyanuric chlorine as previously reported for the preparation of hapten **4d**,[10] introducing the spacer arm on the last step of the synthetic pathway. Thus, hapten **4c** was obtained from **1c**,[10] by sequential nucleophilic substitution with cyclopropylamine and mercaptopropionic acid (see Figure 3, scheme 1). As previously reported,

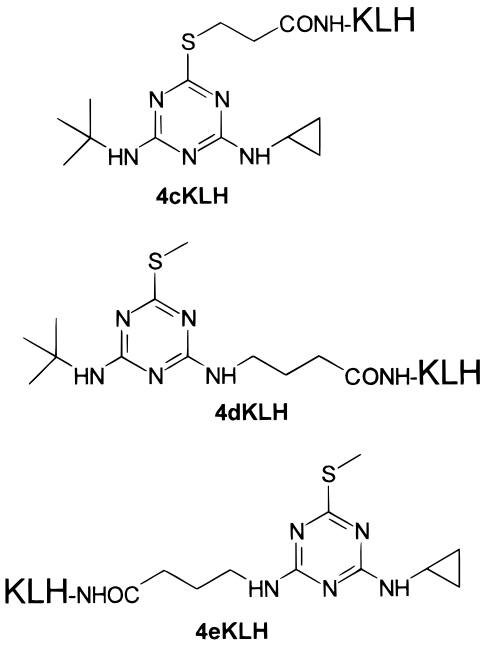

Figure 2. Chemical structures of the three immunizing haptens coupled to KLH. In each hapten, one of the ring substituents of the Irgarol 1051 molecule has been replaced by a spacer arm.

triazine carboxylic haptens containing a sulfur atom showed amphoteric properties that made difficult their isolation and purification from the reaction mixture. We attributed this behavior to the greater ability of the sulfur atom to confer charge to the triazine ring by resonant effect, when compared to that of the chlorine atom. This effect probably causes an increase of the

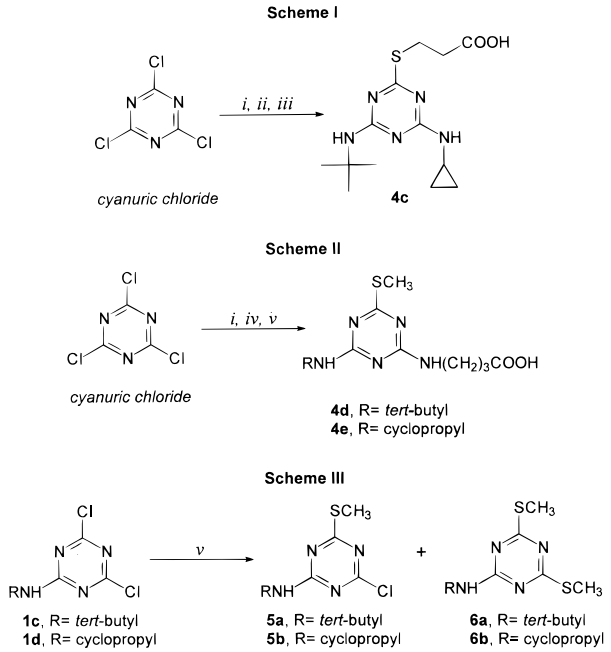

Figure 3. Synthetic pathways used to prepare the immunizing haptens **4c** (scheme 1) **4d**, and **4e** (scheme 2). During the preparation of haptens **4d** and **4e**, attempts to react the intermediates **1c** and **1d**, first with sodium methylthiolate and subsequently with the aminobutyric acid, gave mixtures of the mono- and dimethylthio-substituted derivatives **5a/5b** and **6a/6b**, respectively (scheme 3). Conditions: (i) RNH_2/N(*i*-Pr)$_2$Et, Et_2O, −20 °C; (ii) RNH_2/N(*i*-Pr)$_2$Et, EtOH; room temperature; (iii) $HS(CH_2)_2COOH$, KOH/EtOH, 75 °C; (iv) $H_2N(CH_2)_3COOH$/ N(*i*-Pr)$_2$Et, EtOH; room temperature; (v) $NaSCH_3$/ EtOH, Δ; R = t-Bu or cycloPr.

basicity of the ring that could explain the higher solubility of the S-derivatives in the acidic aqueous media used to precipitate and isolate the other triazine carboxylic haptens. The ^{1}H NMR spectra also evidenced this effect in the smaller chemical shift values of the protons in α position to the amino group of the alkyl substituents. The higher charge density of the ring determines a more electronegatively polarized $C_{triazine}$−N bond to the nitrogen causing a shielding effect on these protons in α. Thus, the protons of the cyclopropyl group of the hapten **4c** appeared at 0.48 and 0.63 ppm, while for its precursor **3c**, with a chlorine atom, the corresponding absorptions showed up at δ 0.54 and 0.76, respectively. Similar effects were observed in other S-substituted triazines when compared with their respective chlorinated derivatives (i.e., **4a** and atrazine; data not shown). Overall, these observations corroborated the convenience of keeping the thioether function on the immunizing hapten.

Hapten **4e** was prepared by replacing one of the chlorine atoms by cyclopropylamine in a first step to obtain **1d**. The aminobutyric acid spacer arm was introduced in a second step, and finally, the methylthio group on the third position of the triazine ring was incorporated (see Figure 3, scheme 2). Attempts to react **1d** with sodium methanothiolate first, introducing the spacer arm in the last step, were unsuccessful. In this case, because of the high nucleophilicity of the thio group a mixture of mono- and disubstituted methylthio derivatives **5** and **6** was obtained (see Figure 3, scheme 3). In contrast, a double nucleophilic substitution of the chlorine atoms was never observed when the amino group was the nucleophile. These compounds were not isolated but were just identified by their chemical shifts in the ^{1}H NMR spectra (δ 2.42, SCH_3 monosubstituted; δ 2.51, 2SCH_3 disubstituted) and by GC/MS according to their retention times (21.03 and 24.68 min) and their molecular ions and fragments in the mass spectra (monosubstituted, m/z 216 one chlorine isotopic pattern; disubstituted, m/z 228 without chlorine isotopic pattern). The same kind of compounds was obtained when **1c** was reacted with sodium methanothiolate to obtain hapten **4d**.[10] Attempts to separate these *tert*-butyl derivatives by normal-phase chromatography led to the corresponding dealkylated amino derivatives because of the acidic properties of the SiO_2 used as stationary phase that promoted the elimination of the *tert*-butyl group.

Haptens **4c**, **4d**, and **4e** were covalently coupled to KLH and used as immunogens to obtain antisera. The yield of the coupling procedure was evaluated on the corresponding BSA derivatives by MALDI-MS (**4c**-BSA, 6.2; **4d**-BSA, 2.7; and **4e**-BSA, 3.1). Despite the low molecular ratio observed, the antisera obtained showed a high antibody titer when tested against the different ETs.

Screening of Competitive Immunoassays. In a direct competitive immunoassay we determine the ability of the analyte to compete with the formation of the HRP tracer−antibody (Ab) complex. Two equilibrium reactions take place simultaneously leading to the analyte−Ab (K_a) and HRP tracer−Ab (K'_a) immunocomplexes. In such assays, the ratio between both affinity constants is the key to obtaining a good immunoassay with very low detection limits. To our knowledge, nobody has made an exhaustive investigation of what should be the optimum value of K_a/K'_a ratio. Affinity constants of polyclonal antibodies cannot usually be adequately assessed due to the heterogeneous multiple specificities. However, this would provide us with significant information for the design of appropriate competitors (haptens that, conveniently attached to an enzyme, could compite with the free analyte for the binding sites of the immobilized antibodies). To solve this lack of information, we screened a battery of 11 HRP tracers with the aim of finding the hapten giving the immunoassay with the best detectability. Simultaneously, we tried to establish some kind of correlation between the chemical structure of the haptens used as competitors and the IC_{50}'s of the immunoassays obtained. The chemical structures of the haptens used for the preparation of ETs are shown in Table 1. We can distinguish four groups of haptens with an increasing degree of structural homology with the target analyte: (i) haptens **2a**−**2d** do have only the triazine ring in common with the irgarol molecule; (ii) haptens **2e**−**2f**, **4a**, and **4b** share with the analyte one of the substituents of the triazine ring; (iii) haptens **4d** and **4e** retain two of the substituents of the irgarol molecule, and finally, (iv) hapten **4c** shows the highest degree of homology with the target analyte. The preparation of these competitors was carried out as previously reported[10,15] and as described in the Experimental Section. The screening for competitive immunoassays allowed evaluation of both the influence of the chemical structure of the immunizing haptens and the quality of the different competitors to provide useful immunoassays.

Influence of the Immunizing Hapten Chemical Structure on the Immunoassay. The competitive immunoassays obtained with each of the combinations and their IC_{50}'s are reported in Table 2. A first look at these results shows that the immunizing

Table 2. IC_{50}'s Obtained When Screening As13−15 (4c-KLH), As16−18 (4d-KLH), and As19−20 (4e-KLH) against 2a−2f, 4a−4e-HRP Tracers for Competitive Immunoassays[a]

Immunogen	Group	HRP-tracer	Antisera IC50s (μg/l) <0.1	0.1...0.3	0.3..1	1..10	>10
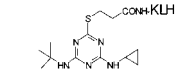 4cKLH		2a		13-14-15			
		2b		13-14-15			
	I	2c		13-	15	14	
		2d		13-15	14		
		2e			13-15	14	
		2f		13-15		14	
	II	4a			13-15	14	
		4b			13-15	14	
	III	4d	15		13-14		
		4e	15		13	14	
	IV	4c		16	16	14	
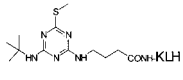 4dKLH		2a		16			17-18
		2b		17	16	18	
	I	2c		17-18	16		
		2d		17	18	16	
		2e		16-17			18
		2f			16-18		17
	II	4a		17	18	16	
		4b		17	18	16	
	III	4d		17	16-18		
		4e			16	17	18
	IV	4c			16	16-17	18
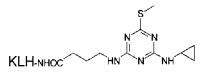 4eKLH		2a				19	20-21
		2b				19	20-21
	I	2c				19	20-21
		2d				19	20-21
		2e				19	20-21
		2f				19	20-21
	II	4a				19	20-21
		4b					19-20-21
	III	4d				19	20-21
		4e					19-20-21
	IV	4c				19	20-21

[a] The gray scale indicates increasing degree of homology with the target analyte Irgarol 1051.

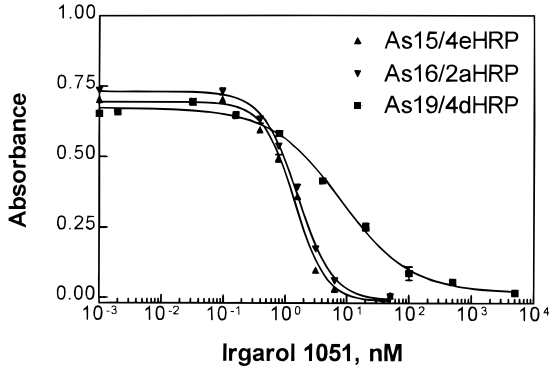

Figure 4. Standard Irgarol 1051 calibration curves of the best competitive immunoassays obtained from each immunizing hapten: **4c**-KLH (As15/**4e**-HRP), **4d**-KLH (As16/**2a**-HRP), and **4e**-KLH (As19/**4d**-HRP). Curves were obtained by following the standard ELISA protocol described in the Experimental Section and using two-well replicates.

haptens **4c** and **4d** gave the best antisera. Both of them provided, already in the screening step, several useful competitive immunoassays with acceptable IC_{50}'s. Hapten **4c** gave the highest number of assays with great detectability. Any of the combinations afforded immunoassays with IC_{50}'s higher than 10 μg/L. In contrast, the immunizing hapten **4e** did not yield any useful immunoassay; only As19 was able to afford some assays showing IC_{50} values close to 1 μg/L, which is insufficient for direct trace analysis although the detectability could perhaps have been improved by varying the immunoassay conditions.

In light of these results, we intended to find an explanation for the low quality of the immunizing hapten **4e** when compared to **4c** and **4d**. Considering the difference of behavior of hapten **4e** as an immunizing hapten, it seems clear that the *tert*-butyl group, which is absent in this molecule, must be the most important antigenic determinant of the analyte. In contrast, despite the also important steric magnitude of the cyclopropyl group (see Figure 1A), this group seems to have minimum participation in stabilizing the immunocomplexes. We compared the MM+ optimized geometries of these haptens and the irgarol molecule (see Figure 1) and attempted to evaluate the noncovalent interactions that could participate in the stabilization of the analyte−antibody immunocomplexes in each case. Figure 1B−D exhibits the optimized geometries of the haptens. The more stable conformer of hapten **4c** shows the greatest structural similarity with the analyte; the potential binding interactions commented above are nearly equal (see Figure 1A and B). However, with small differences, both immunizing haptens **4c** (with cyclopropyl group) and **4d** (without this substituent) gave a very similar number of competitive immunoassays (see Table 2). Therefore, although hapten **4c** could be selected as the best immunizing hapten, **4d** seems to keep most of the important structural features of the irgarol molecule. Regardless of the absence of the cyclopropyl group, the spacer arm partially imitates this group when the nitrogen−alkyl angle is considered (see Figure 1A and C), being the NH group free to establish hydrogen bonds with the antibodies while showing similar asymmetric ring facial distribution.

The decrease of the antisera avidity for the target analyte when the *tert*-butyl group was absent from the chemical structure of the immunizing hapten **4e** has been explained by several criteria (see Figure 1A and D). The *spatial atom geometry* of hapten **4e** is very different from that of the analyte, with a lower steric volume and restrictions. On the other hand, the absence of the bulky *tert*-butyl group causes a lack of *hydrophobic interactions*. Thus, the antibodies obtained are not able to stabilize the immunocomplex by establishing hydrophobic interactions with this important hydrophobic area of the Irgarol 1051 molecule. Finally, the *hydrogen-bonding* capabilities are not equal for hapten **4e** and Irgarol 1051. The antibodies produced are prone to establish equal hydrogen bonds with both NH groups, which are equally accessible in this hapten, but not in the Irgarol 1051, where one of them is less accessible because of the steric hindrance caused by the presence of the *tert*-butyl group.

After all the above-mentioned considerations, we conclude that the As raised against immunizing haptens possessing the *tert*-butyl group are able to establish more efficient interactions with the analyte. This fact explains the greater number of immunoassays showing sufficient detectability for the anaysis of trace levels of Irgarol 1051 in environmental seawater samples.

Influence of the Chemical Structures of the ETs on the Immunoassay. As we mentioned above, the sensitivity of the immunoassay is highly dependent on the ratio of the affinity constants participating in the equilibria. Looking at the IC_{50}'s obtained for a single immunogen and the 11 HRP tracers screened, it can be observed that the chance of obtaining an assay with high detectability are greater if the chemical structure of the ET differs to a high extent from that of the analyte, especially for low-avidity antisera. Thus, the number of antisera giving usable assays is higher when the analogy of the ET is lower (groups I and II). For example, the three antisera (As13, As14, and As15;

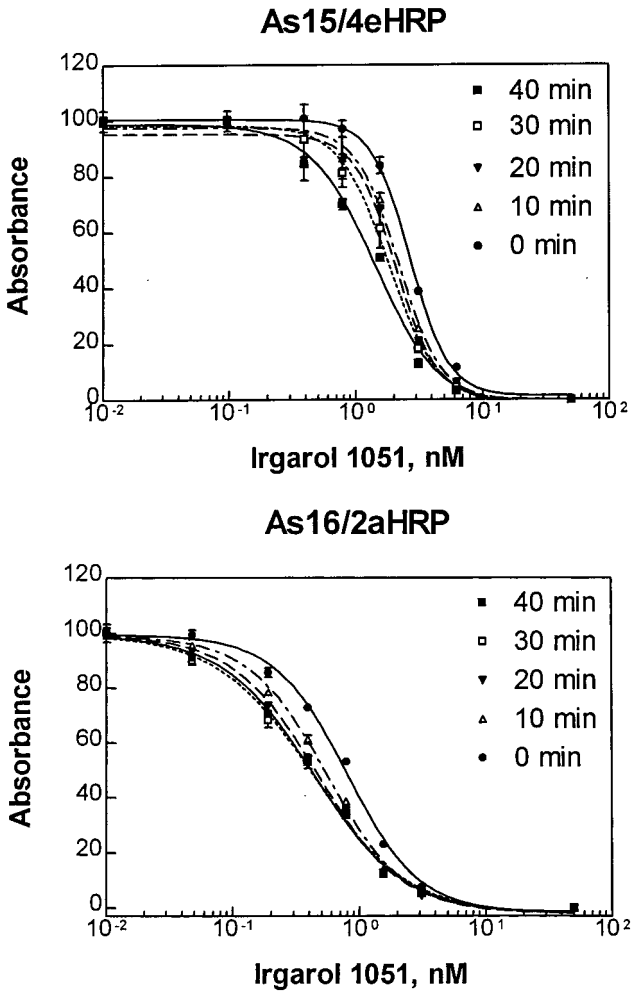

Figure 5. Effect of preincubating the analyte on the antibody-coated plates during different periods of time using the immunoassays As15/**4e**-HRP and As16/**2a**-HRP. An increase of the incubation time enhanced the detectability of the immunoassay. For each As/ET combination, ELISAs were carried out in three separate plates each of them containing two-well replicate curves of the analyte incubated on the antibody-coated plates during periods of 0, 10, 20, 30, and 40 min.

see Table 2) obtained when immunizing with **4c**-KLH are able to give useful assays (IC_{50}'s 0.1−0.3 μg/L) with ETs from group I; As13 and As15 also do it with ETs from group II, and finally, only As15 is able to afford assays if the competitors belong to groups III and IV. As14, showing the lowest titer of the group, was only able to give assays with IC_{50} lower than 1 μg/L, if the ETs were from group I. Similarly, when the immunizing hapten was **4d**-KLH, the three As raised were able to provide useful competitive immunoassays when the tracers belong to group I, but only As17 was able to give assays showing enough detectability with the competitors from groups II, III, and IV (see Table 2). In contrast, for As with high avidity for the analyte, we hypothesize, although it should be proved with other antisera, that it is possible to obtain good assays even under homologous or quasi-homologous conditions (see the behavior of As15 and As17 in Table 2).

It is worth noting the lower value of the slopes of the immunoassays developed with the antisera raised against **4d**-KLH (average slope values for As16 1.1 ± 0.41, As17 0.69 ±0.11, and As18 0.86 ± 0.22). In contrast, the slopes of most of the competitive immunoassays using antisera raised against **4c**-KLH, had values higher than 1 (average slope values for As13 1.06 ± 0.16, As14 0.97 ± 0.15, and As15 1.91 ± 0.43). High slope values have been often associated with high-affinity antibodies, which is in agreement with the higher structural homology of the immunizing hapten **4c** and Irgarol 1051. Figure 4 shows the calibration graphs of the As/ET combinations selected for each of the three immunogens evaluated. It can be observed how the best immunoassay obtained with the antisera raised against **4e**-KLH (As19/**4d**-HRP) does not reach the necessary detection limit although it shows a good slope and A_{max}/A_{min} ratio.

Table 3. Effect of the Ionic Strength in the Immunoassay Parameters[a]

PBS, M	n	A_{max}	A_{min}	IC_{50}, pM	slope	R^2
0.02	4	0.707 ± 0.051	0.001 ± 0.001	295 ± 31	1.9 ± 0.1	0.995
2	6	0.630 ± 0.041	0.007 ± 0.005	330 ± 32	1.2 ± 0.1	0.989

[a] A_{max}, A_{min}, IC_{50}, and slope are the parameters *A*, *B*, *C*, and *D*, respectively, of the four-parameter logistic equation used to fit the standard curves (see Experimental Section). The values shown were obtained with the immunoassay AS15/**4e**-HRP and are the average of n calibration curves run on two separate ELISA plates.

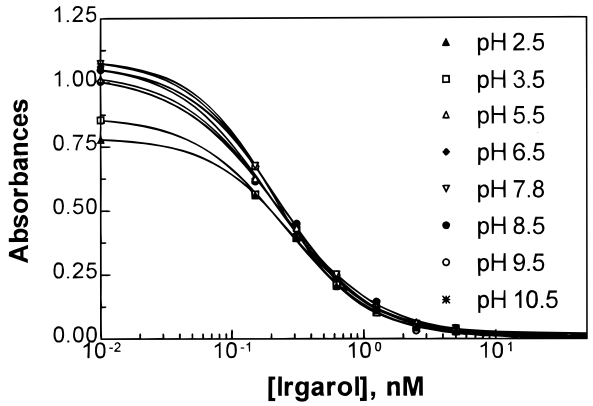

Figure 6. Effect of the pH on the immunoassay As16/**2a**-HRP. The ELISA is operative between pH 2.5 and 10.5. Only a small decrease in detectability and maximal absorbance was observed at acidic pHs whereas no significant changes occurred at basic pHs (see text for details). Assays were run simultaneously on three different ELISA plates.

Immunoassay Optimization and Evaluation. Immunoassays As15/**4e**-HRP and As16/**2a**-HRP were selected for further optimization and evaluation of the immunoassay protocol. Several parameters were studied such as incubation time, ionic strength, and pH. From all of them, the incubation time was the most determinant to improve immunoassay detectability. In these studies, Irgarol 1051 was incubated on the antibody-coated plates during increasing periods of 0, 10, 20, 30, 40, and 50 min before adding the ET, which was subsequently incubated for 60, 50, 40, 30, 20, and 10 min, respectively (competitive step). This strategy has proved to be useful for other assays developed in this[15] and other laboratories.[17] Figure 5 shows the shift of the calibration curves for the immunoassays investigated. Both immunoassay combinations showed the same behavior: a preincubation of the analyte with the antibody and reduction of the competitive step

(17) Weller, M. G.; Weil, L.; Niessner, R. *Mikrochim. Acta* **1992**, *108*, 29−40.

Table 4. Parameters of the Optimized ELISAs for Irgarol 1051[a]

assay	*n*	A_{max}	A_{min}	IC_{50}, pM	slope	working range, pM	LOD, pM
As15/**4e**-HRP	9	0.742 ± 0.045	0.007 ± 0.079	293 ± 79	1.7 ± 0.3	114−668	63 ± 24
As16/**2a**-HRP	4	0.867 ± 0.161	0.019 ± 0.009	304 ± 83	1.3 ± 0.1	110−848	62 ± 14

[a] A_{max}, A_{min}, IC_{50}, and slope are the parameters *A*, *B*, *C*, and *D*, respectively, of the four-parameter logistic equation used to fit the standard curves (see Experimental Section). The values shown for As15/**4e**-HRP correspond to the average of nine curves run on three separate plates simultaneously. The values shown for As16/**2a**-HRP correspond to four curves run on four separate plates on two different days. The working range was determined by the concentration values giving 80 and 20% of the control zero absorbance. The LOD is the concentration producing 90% of the control zero absorbance.

Table 5. Selectivities of the Immunoassays Obtained against the Immunogens 4c-KLH, 4d-KLH, and 4e-KLH

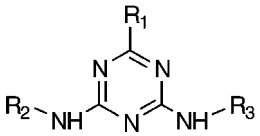

				As15/**4e**-HRP		As16/**2a**-HRP		*As17/**4b**-HRP*	As19/**4d**-HRP	
analyte	R_1	R_2	R_3	IC_{50}, nM	CR, %	IC_{50}, nM	CR, %	*CR, %*	IC_{50}, nM	CR, %
Irgarol 1051	SCH_3	*tert*-butyl	cyclopropyl	0.325 ± 0.075	100	0.244 ± 0.098	100	*100*	1.79 ± 0.35	100
terbutryne	SCH	*tert*-butyl	ethyl	0.34	88	2.25	14	*148*	20.8	8
terbumeton	OCH_3	*tert*-butyl	methyl	0.49	52	nd[a]	nc[b]	*18*	35.8	5
tertbutylazine	Cl	*tert*-butyl	ethyl	1.31	29	nd	nc	*10*		nc
prometryne	SCH_3	isopropyl	isopropyl	2.75	15	0.49	45	*8*	0.71	305
ametryne	SHC_3	isopropyl	ethyl	3.37	12	2.42	9	*8*	2.34	92
desmetryne	SCH_3	isopropyl	methyl	6.31	6	nd	nc	*nc*	6.25	34
propazine	Cl	isopropyl	isopropyl	7.68	5	4.39	3.5	*15*	6.78	21
atrazine	Cl	isopropyl	ethyl	7.37	3	nd	nc	*5*	8.89	16
cyanazine	Cl	$C(CN)(CH_3)_2$	ethyl	2.46	13	nd	nc	*8*	594	0.2
simazine	Cl	ethyl	ethyl	15.17	3	nd	nc	*3*	27.6	5.2

[a] nd, not detected at concentrations below 100 nM. [b] nc, not cross-reacted.

period improved immunoassay detectability. Incubation periods of 15−20 min for the competitive step were chosen as a compromise between detectability and maximal absorbance of the assay.

Ionic Strength. This was considered an important physical parameter to study since this immunoassay was addressed to analyze seawater samples with a high salinity content. To evaluate the influence of the ionic strength on the immunoassay features, assays were carried out at increasing PBS concentrations varying from 0.2 to 2 M. Table 3 shows how the immunoassay parameters were not significantly changed by increase of the salt content of the buffers, except for a slight diminution of the maximal absorbance and a decrease of the slope value. In light of this result, 0.2 M PBS was selected for further experiments.

pH Effect. Similarly, the immunoassay reported in this paper is stable under a very broad range of pH. Figure 6 shows the calibration graphs obtained by varying the pH of the assay buffer from 2.5 to 10.5. Only a small decrease of the sensitivity and of the maximal absorbance was observed at acidic pH ($n = 3$, IC_{50} 90 ± 34 and 80 ± 15 ng/L; A_{max} 0.794 and 0.878, for pH 2.5 and 3.5, respectively) when compared with the assay parameters at pH 7.8 ($n = 4$, IC_{50} 76 ± 21 ng/L; A_{max} 1.102). From pH 5.5 to basic pH, the immunoassay parameters did not differ significantly ($n = 3$, IC_{50}'s 73 ± 23 and 75 ± 29 ng/L; A_{max} 1.046 and 1.096 for pH 5.5 and 10.5, respectively).

Table 4 summarizes the parameters defining the calibration graph of the optimized immunoassays As15/**4e**-HRP and As16/**2a**-HRP. Both immunoassays show a good signal and an excellent sensitivity. The only difference is the high value of the slope of the immunoassay As15/**4e**-HRP that produces a narrower working range. Immunoassay As16/**2a**-HRP with a slope of 1.34 confers enough precision while it broadens the range of concentrations that can be measured.

Immunoassay Specificity. The immunoassays obtained with the three immunogens were evaluated according to their selectivity versus other structurally related compounds. The results are summarized in Table 5. With the As15/**4e**-HRP, the importance of the *tert*-butyl group for antibody recognition was again noted. These triazine herbicides possessing a methylthio group in their structure are only slightly recognized in this system (i.e., prometryne 15%); however, the *tert*-butyl group constitutes a stronger antigenic determinant (i.e., terbutylazine 29%). As a consequence, the best recognized triazines are those possessing both of the above groups (i.e., terbutryn 88%). The cross-reactivities obtained could map the recognition elements for each Ab/ET pair. As an example, structural and electronic features of terbumeton, prometryne, and propazine were analyzed by molecular modeling, compared to those of irgarol, and related to the observed cross-reactivity values. In electronic terms, only the change of the methylthio group for a chlorine atom or a methyloxy group modifies the net charge of the triazine ring and the electronic distribution but not the net dipolar moment of the molecule. The isopropylamino group (propazine and prometryne) partially mimicked the steric and hydrophobic properties of the *tert*-butyl group, although its conformational restrictions are lower and all the main conformers could be equally populated.

Surprisingly, the immunoassay As16/**2a**-HRP was the most specific for Irgarol 1051. Regardless of the presence of the *tert*-

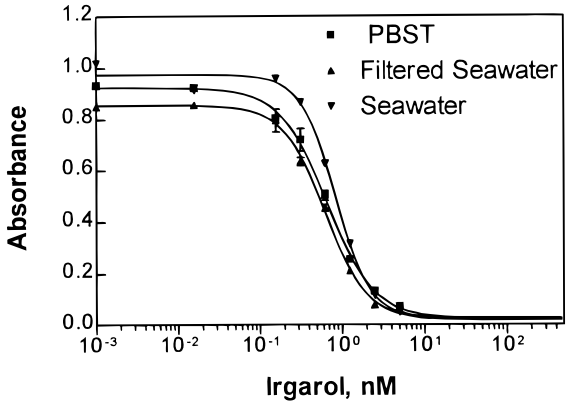

Figure 7. Effect of the seawater matrix in the ELISA As15/**4e**-HRP. Seawater collected from the open sea to ensure the absence of the analyte was split in two fractions and one of them was filtered before its use to prepare the standard curve. Assays were carried out on two separate plates using three-well replicates.

Table 6. Acuracy of the Assay[a]

sample	spike level, nM	*n*	measured, nM	recovery, %
seasalt water	0.2	2	0.27 ± 0.11	135
	0.4	2	0.37 ± 0.06	93
	0.6	3	0.61 ± 0.06	101
	0.8	3	0.98 ± 0.12	122
	1.5	6	1.41 ± 0.35	94
Malvarosa	3.98	2	4.35 ± 0.07	109

[a] Spiked water samples were buffered measured in the ELISA 2- and 4-fold diluted using two-well replicates.

butyl and the *S*-methyl groups on the chemical structure of the immunizing hapten, a pesticide such as terbutryne containing both groups was only slightly recognized, while terbumeton and terbutylazine did not cross-react at the concentrations studied (up to 100 nM). Until now we have not found any explanation for this behavior other than animal variability. In contrast, the immunoassay As17/**4b**-HRP, raised against the same immunogen showed the expected selectivity (see Table 5, *italics*).

Finally, immunoassay As19/**4d**-HRP, recognizes best those analytes possessing *S*-methyl and -isopropyl groups, such as prometryne (305%) or ametryne (92%). Probably the isopropyl group can mimic the cyclopropyl group of the immunizing hapten, thus explaining the high extent of recognition of the pesticide prometryne with two isopropyl groups in its chemical structure. The presence of the bulky *tert*-butyl group in pesticides such as terbutryne or terbutylazine reduces drastically the recognition, despite the presence of the *S*-methyl and -ethyl groups that could also mimic the spacer arm of the hapten **4e**. The reasons are probably the same as those mentioned above for the lack of recognition of Irgarol 1051 by these antibodies.

Effect of a Seawater Matrix. Seawater was collected from the open sea to ensure the absence of the analyte. One fraction was filtered before its use in the ELISA. The studies demonstrated that seawater does not significantly affect immunoassay performance; however, because of the slightly larger absorbance observed at low concentration values, measurements carried out without filtering the sample may underestimate irgarol concentration in environmental samples. In contrast, no effect of the matrix

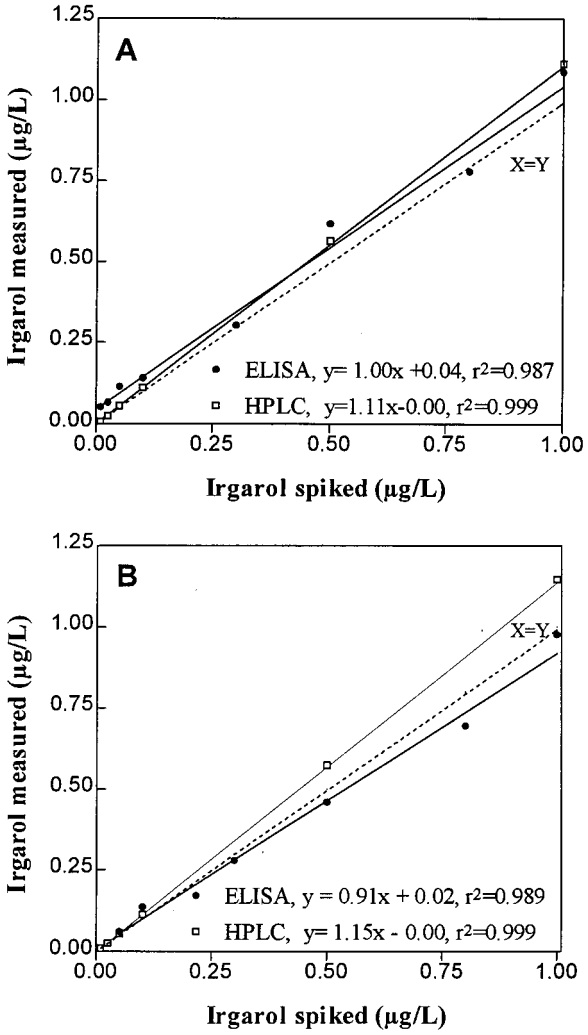

Figure 8. Accuracy studies to assess the correlation between HPLC/DAD and ELISA measurements using spiked MilliQ water samples (A) and seasalt water samples (B). Whereas the slopes were very close to 1 for water samples, a slight bias was observed in both analytical techniques in the presence seasalts. ELISA analyses were carried out using two-well replicates of 1-, 2-, and 4-fold PBST-diluted water samples.

was observed if seawater was filtered just before the ELISA analysis (see Figure 7).

The *accuracy* of the assay was studied by spiking water samples at different levels (0.2−1.5 nM). In this experiment, the recoveries obtained were always close to 100% (see Table 6). Similarly, we compared the optimized ELISA with HPLC/DAD by measuring spiked MilliQ and seawater samples. The correlation obtained between spiked and measured concentrations was always good, and the slope of the linear regression equations was close to 1 in both techniques (ELISA 1.00; HPLC 1.11) when measuring spiked MilliQ water (see Figure 8, A). The slope was lower (slope 0.91) when ELISA measurements were performed on spiked artificial seawater samples which is in agreement with the matrix effect previously mentioned (see Figure 8B). However, it must also be noted that a slight bias in the oposite direction was also observed for the chromatographic results (slope 1.15). When analyzing the goodness of the correlation between the HPLC and the ELISA results, the regression coefficients (r^2) were 0.999 and 0.996, and the standard deviations of the residuals ($Sy{\cdot}x$) 0.02 and 0.03 for

Table 7. Results from the Analysis of Irgarol 1051 in Real Seawater Samples[a]

sample	ELISA, pM	HPLC/DAD, pM
Masnou (4/96)	>668	1284[b]
Masnou (8/96)	<LOD	86[b]
Masnou (1/97)	<LOD	12[b]
Cullera	<LOD	<LOD
Malvarosa	<LOD	<LOD
Jucar river (7/97)	<LOD	<LOD
Jucar river (9/97)	254	278
Jucar river (10/97)	209	nt[c]

[a] The samples were buffered and analyzed 2- and 4-fold diluted by ELISA (As15/**4e**-HRP). [b] Results reported by Ferrer et al.[8] The LOD of the ELISA method is 63 ± 24 pM; the LOD of the HPLC method is 0.5 pM. [c] nt, not tested.

the MilliQ ($y = 0.94x + 0.05$) and the seasalt ($y = 0.82x + 0.02$) water samples, respectively.

Finally, *real samples* were collected and measured with the optimized immunoassay As15/**4e**-HRP and the results compared with those obtained by HPLC/DAD (Table 7). The only treatment applied to the water samples prior to the analysis was filtering of the water and adding a small amount of PBS buffer. The results obtained matched very well those obtained by the chromatographic method. These results also show that Irgarol 1051 may be a ubiquitous contaminant of coastal waters of the Mediterranean as was pointed out in previous studies.[3,5,8]

CONCLUSIONS

To rationalize hapten design and immunoassay development, in this paper we have studied the participation of the different antigenic determinants of the irgarol molecule on eliciting antibodies. High antiserum avidities are desirable to develop sensitive immunochemical techniques able to detect environmental pollutants at the trace level. Since antibody recognition is based on the establishment of noncovalent interactions, it is evident that the chemical structure and electronic distribution of the target analyte plays an important role. The immunizing hapten analyte should preserve these features although the location of the spacer arm introduces certain variations. Chemical conjugation of the irgarol molecule to carrier proteins needs to replace one of the ring substituents to introduce an appropriate linker. The evaluation of the antisera obtained against the three immunizing haptens prepared, **4c**, **4d**, and **4e**, has revealed that the cyclopropyl group does not really play an important role in stabilizing the immunoclomplex. In fact, the antiserum obtained against hapten **4d** shows a high avidity comparable to **4c** where all the original substituents are present. On the other hand, hapten **4e** has yielded antisera with poor recognition of the irgarol molecule. These results have been interpreted by considering the more favored conformations adopted in aqueous solutions by the analyte and the three haptens studied. The present paper demonstrates that high-quality antibodies can be anticipated by molecular modeling studies of the analyte conformations and of the immunizing hapten geometries, hydrogen-bonding capabilities, and electronic distributions. Similarly, we show how sensitivity and detectability requirements of competitive immunoassays can be modulated by selecting the appropriate chemical structure of the hapten to be coupled to the enzyme. We have selected the two best antisera (As15 and As16) from the two best immunogens (**4c**-KLH and **4d**-KLH, respectively) and developed direct competitive ELISAs reaching very low limits of detection. These assays have been optimized and evaluated in terms of effect of selected physicochemical conditions, selectivity, accuracy and performance on seawater matrixes. Because of their simplicity, sensitivity, selectivity and high-throughput sample processing, the immunoassays presented here have proven to be useful tools to carry out monitoring studies of the contamination by the antifouling agent Irgarol 1051 in coastal areas.

ACKNOWLEDGMENT

This work has been supported by the EEC Environment Program (Contracts ENV4-CT95-0066 and ENV4-CT97-0476), "ACE" MAST-III (PL-971620) and CICYT (AMB96-7808-CE and AMB98-1048-C04-01). We thank Dr. Josefina Casas (Animal Breeding Facility, C.I.D.—C.S.I.C.), Dr. Oriol Bulvena, M-Angeles García, and Manel Gonzalez (Laboratorios Viñas, Barcelona, Spain) for their kind assistance in animal treatments and Ciba-Geigy (Barcelona, Spain) for supplying samples of simazine, atrazine, and Irgarol 1051.

Received for review March 4, 1998. Accepted June 18, 1998.

AC980241D